# Copyright Warning & Restrictions

The copyright law of the United States (Title 17, United States Code) governs the making of photocopies or other reproductions of copyrighted material.

Under certain conditions specified in the law, libraries and archives are authorized to furnish a photocopy or other reproduction. One of these specified conditions is that the photocopy or reproduction is not to be "used for any purpose other than private study, scholarship, or research." If a, user makes a request for, or later uses, a photocopy or reproduction for purposes in excess of "fair use" that user may be liable for copyright infringement,

This institution reserves the right to refuse to accept a copying order if, in its judgment, fulfillment of the order would involve violation of copyright law.

Please Note: The author retains the copyright while the New Jersey Institute of Technology reserves the right to distribute this thesis or dissertation

Printing note: If you do not wish to print this page, then select "Pages from: first page # to: last page #" on the print dialog screen

## ABSTRACT

## CHEMICAL VOLATILIZATION OF HEAVY METALS FOR WASTE SEPARATION AND REAL TIME METALS ANALYSIS

by
**Mohammad Nasr Ul-Alam**

One of the major challenges in environmental analysis concerns the rapid and sensitive detection of metals emitted from combustion stacks. An interesting concept for real time analysis is to convert airborne metal oxide particles in a flow reactor into relatively volatile compounds of a single class, and then analyze in the gas phase. In this project, kinetics of chemical volatilization reaction between $Sb_2O_3$ and HCl was investigated. To achieve this a laboratory volatilization flow reactor was built and data was collected for the volatilization reaction in terms of conversion, inlet and outlet concentrations and flow rates. A mathematical model was also developed to regress the data to find the kinetic parameters for this reaction.

It was shown by the experimental results that by varying HCl rate and keeping dust rate constant, there was no marked effect on conversion and it almost remained constant. But the volumetric rate of $N_2$ will definitely effect conversion. Also by increasing reactor set point temperature from 300C to 400C, a significant increase in conversion was observed The data and kinetic parameters obtained from this project are important for facilitating the design of an airborne metal CEM and enhancing metals detection.

# CHEMICAL VOLATILIZATION OF HEAVY METALS FOR WASTE SEPARATION AND REAL TIME METALS ANALYSIS

by
Mohammad Nasr Ul-Alam

A Master's Thesis
Submitted to the Faculty of
New Jersey Institute of Technology
In Partial Fulfillment of the Requirements for the Degree of
Master of Science in Chemical Engineering

Department of Chemical Engineering, Chemistry and Environmental Sciences

August 1999

## APPROVAL PAGE

## CHEMICAL VOLATILIZATION OF HEAVY METALS FOR WASTE SEPARATION AND REAL TIME METALS ANALYSIS

**Mohammad Nasr Ul-Alam**

---

Dr. Robert Bob Barat, Advisor — Date
Associate Professor of Chemical Engineering, NJIT

---

Dr. Robert Pfeffer, Committee Member — Date
Distinguished Professor of Chemical Engineering, NJIT

---

Dr. Dana Knox, Committee Member — Date
Associate Professor of Chemical Engineering, NJIT

## BIOGRAPHICAL SKETCH

**Author:** Mohammad Nasr Ul-Alam

**Degree:** Master of Science in Chemical Engineering

**Date:** August 1999

**Undergraduate and Graduate Education:**

- Master of Science in Chemical Engineering,
  New Jersey Institute of Technology, Newark, NJ, 1999
- Bachelor of Science in Chemical Engineering,
  University of the Punjab, Lahore, Pakistan, 1997

**Major:** Chemical Engineering

To my beloved family

## ACKNOWLEDGMENT

I would like to express my deepest appreciation to Dr. Robert Bob Barat, who not only served as my thesis advisor, providing valuable and countless resources, insight and intuition, but also constantly gave me support, encouragement, and reassurance. Special thanks are given to Dr. Robert Pfeffer and Dr. Dana Knox for actively participating in my committee.

## TABLE OF CONTENTS

## TABLE OF CONTENTS
## (Continued)

**Chapter** **Page**

## LIST OF TABLES

## LIST OF TABLES
## (Continued)

**Table** **Page**

## LIST OF FIGURES

# CHAPTER 1

# INTRODUCTION

## 1.1 Background Information

One of the major challenges in environmental analysis concerns the rapid and sensitive detection of metals emitted from combustion stacks. Metal effluents from incinerators consist primarily of metal oxide particles, and metal halide particles and vapors. Minor constituents includes metal hydroxides (solids and vapors), organometallics (generally vapors), metal carbonates, metal sulfides, and miscellaneous salts and compounds. In addition to homogeneous particles, metal compounds also appear adsorbed to inorganic particulates (silicas and aluminas) and soot.

The emission of airborne submicron metal particles of many different forms imposes severe difficulties on real time analysis, including: matrix effects and interferences, possibility of incomplete digestion, lack of suitable calibration standards, inability to preconcentrate the sample, and poor sample transport to the detector.

An interesting concept for real time analysis that solves some of these difficulties has airborne metal oxide particles (non-volatile) converted in a flow reactor into relatively volatile compounds of a single class, and then analyzed in the gas phase. A promising conversion scheme for metals volatilization involve chlorine displacement of oxygen, sulfur or carbonaceous ligands [4]; e.g.,

$$MO + 2HCl \rightarrow MCl_2 + H_2O$$

$$MS + 2HCl \rightarrow MCl_2 + H_2S$$

$$M - CO + NH_4Cl \rightarrow HMCl + CO + NH_3$$

where M= Metal , such as As, Sb, Hg, Cd, and other toxics. These reactions are generally exothermic (see table 1.1) due principally to the high electronegativity of chlorine, which results in the very strong M-Cl bond [4].

**Table1.1** Heats of formation of metal Chlorides [4]

| Compound | $\Delta H_{298}$ Kcal/mol |
|---|---|
| $AsCl_3$ | -80.2 |
| $CdCl_2$ | -92.149 |
| $HgCl_2$ | -53.4 |
| $SbCl_3$ | -91.3 |

In general , metal chlorides are more volatile than parent metals, oxides, hydroxides, and sulfides. This makes them ideal candidates for gas phase analysis.

**Table 1.2** Required Temperatures for corresponding vapor pressures of selected metal Oxides and chlorides [8]

| Compound | For 20mm Hg C | For 40mm Hg C | For 60mm Hg C | For 100mm Hg C |
|---|---|---|---|---|
| $As_2O_3$ | 279.2 | 299.2 | 310.3 | 332.5 |
| CdO | 1200 | 1257 | 1295 | 1341 |
| $Sb_2O_3$ | 729 | 812 | 873 | 957 |
| $AsCl_3$ | 36 | 50 | 58.7 | 70.9 |
| $CdCl_2$ | 695 | 736 | 762 | 797 |
| $SbCl_3$ | 100.6 | 117.8 | 128.3 | 143.3 |

By converting metal species into metal chlorides, one can achieve a far more uniform chemical environment. This will dramatically ease the calibration burden; the detector can be calibrated on pure compounds of the elements to be determined without the need for matrix-matched reference materials. The technique eliminates interferences from both matrix elements and atomizing media. The improvement in transport of metals to the detector by using a volatilization unit should result in an enhancement of sensitivity, by reducing losses from condensation or reaction of complex low volatility species in the detector feed lines.

The quantitative conversion of airborne metal oxide particles into volatile metal halides would enhance the functionality of a proposed airborne metals continuous emission monitor (CEM), such as shown in Figure1. An extractive probe would feed stack gas through an inertial filter. Airborne particles are separated and flowed through the halogenation reactor. All metal vapors would then flow into a laser-based analyzer, which uses photofragment fluorescence [9]. With continuous data on stack metals, feedback control to the incineration process is possible.

Proof of concept has already been established by performing experiments in a simple reactor [10]. Metal Oxide particles were placed on a quartz frit in a flow tube suspended vertically in a one zone tube furnace. Metered dilute HCl gas (in $N_2$) was flowed downward past the static particles. Volatile metal chloride product was captured in a cold trap for off-line analysis in a flame atomic absorption analyzer. In testing with $Sb_2O_3$, nearly quantitative oxide conversion and chloride recovery were achieved. Condensed $SbCl_3$ was collected and analyzed after each run. The total mass of collected Sb was within 12% of the total starting mass of Sb. This proved that conversion definitely

occurred at reasonable temperatures, thus suggesting that the volatilization concept is valid.

## 1.2 Objective

While the thermodynamics for the halogenation reactions are well established, little is known concerning the kinetics of such gas/solid reactions. The overall objective of this project is to identify and optimize a chemical reaction sequence which quantitatively converts metal compound particulates into volatile metal derivatives in a flow reactor configuration. To achieve this, data have been collected for the reaction between Antimony Oxide($Sb_2O_3$) and gaseous HCl, and mathematical modelling has been done. These data and the model are used together to estimate the kinetic parameters of reaction. These technical data will also be valuable in the development of a sample treatment chamber as the front end of an analytical instrument for real-time stack gas airborne metals monitoring.

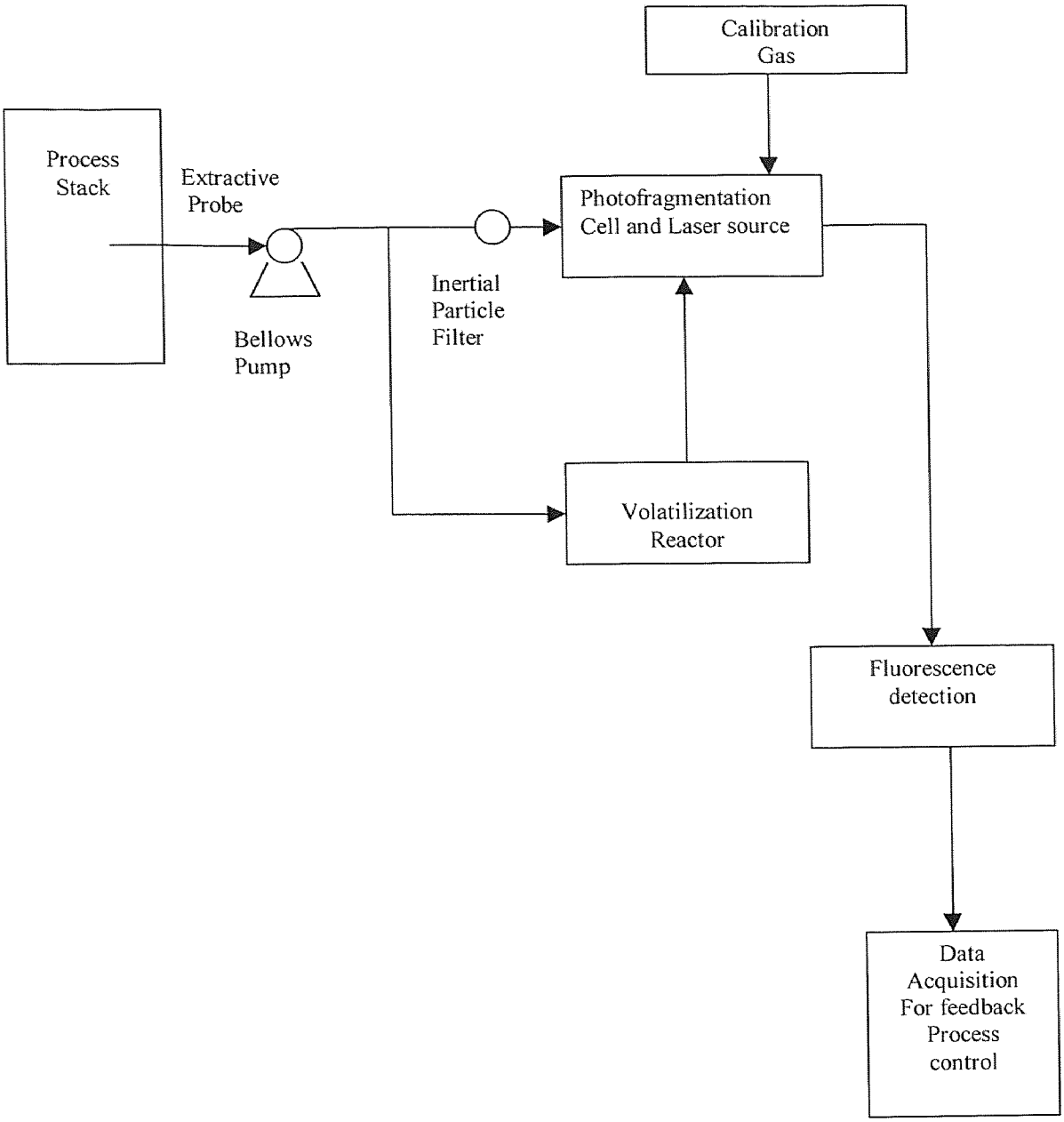


**Figure1** Proposed Metals CEM Technology

# CHAPTER 2

# EXPERIMENTAL

## 2.1 Experimental Setup

The test apparatus for this project is shown in Figure 2.1. A Wright commercial laboratory dust feeder model WDF-II [9], packed hard with <5 micron $Sb_2O_3$ particles, is used to introduce the metal oxide particulates into a metered, fixed entraining nitrogen flow(1.5 SCFM). By varying the mechanical dust generation rate, a wide range of particulate mass concentrations can be produced.

In order to have flexibility in varying reactor residence times, a portion of the dust-laden flow is vented. The flow to the reactor is monitored with a calibrated venturi meter, which was constructed on site. Unlike a rotameter, the venturi meter is not subject to clogging or fouling due to oxide dust.

The flow reactor itself is a quartz tube of ¼ inch diameter, located inside a three- zone furnace. The three zones are independently temperature controlled in an attempt to achieve isothermal conditions throughout much of a reactor. Three thermocouples provided feed back to the temperature controllers. These thermocouples, however, are external to and not in contact with the reactor tube. The small tube diameter reduces any radial temperature dependance.

Two glass bubblers containing standardized NaOH solution and Phenolphthalene indicator are set at the outlet of the reactor, through which reactor effluent is bubbled and then passed to the vent. Temperature controlled heating tape is wrapped on the

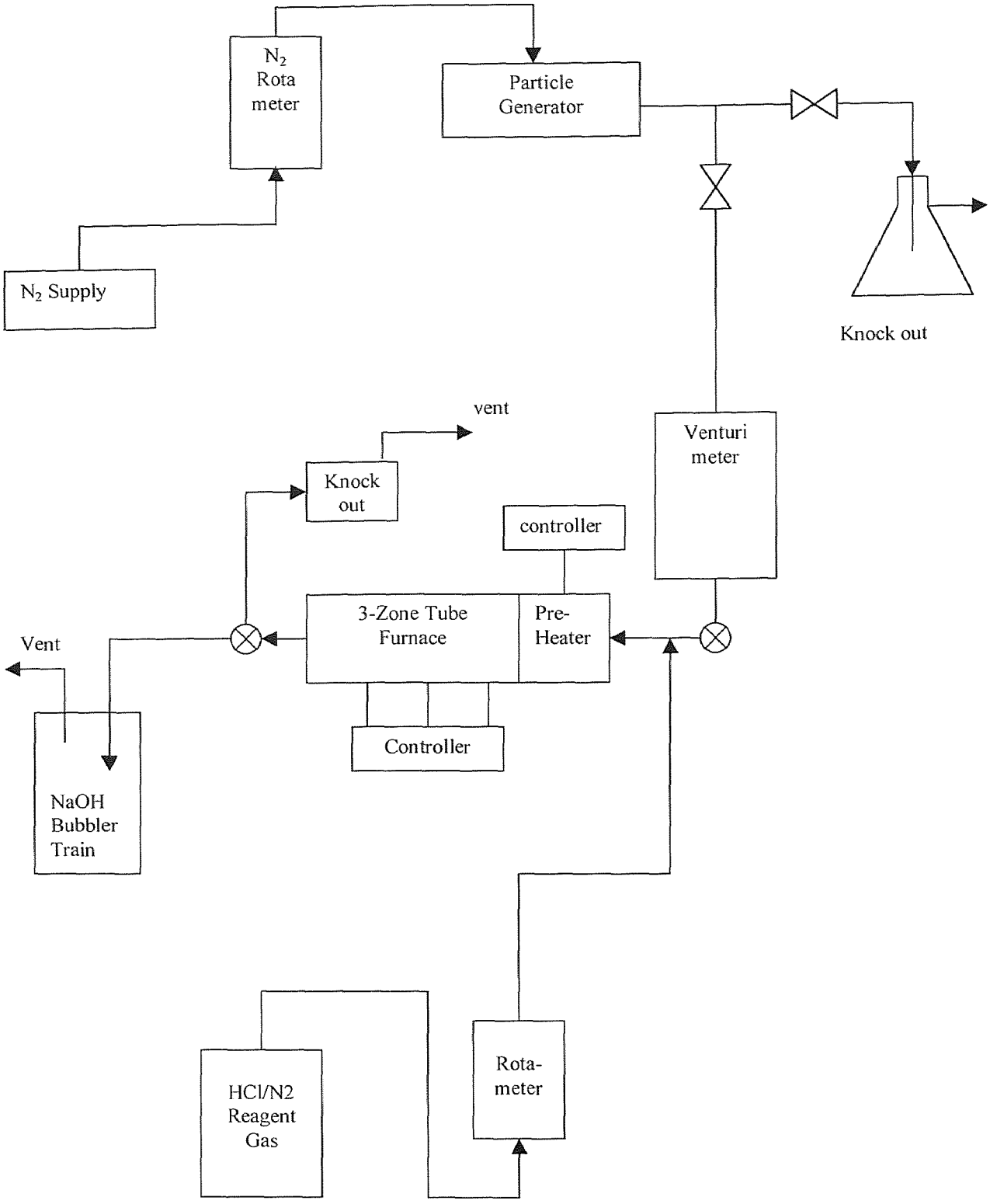


**Figure 2.1** Chemical Volatilization Experimental Apparatus

outlet line between reactor and bubblers in order to keep the temperature above the dew point of HCl. A point of interest here lies in the choice of $N_2$ instead of air as the carrier gas. It was observed that bubbling air through the NaOH solutions caused their neutralization to end point. This was due to the ambient $CO_2$ in the air dissolving in the basic solutions.

A small, temperature controlled, one zone furnace provides some preheat to the flow before the main furnace. Axial temperature profiles along the inside of the reactor tube were obtained by sliding a thin thermocouple down the reactor tube length.

## 2.2 Experimental Work and Results

The reservoir cup of the dust feeder was filled with a fine dust (<5micron, 99+ %) of $Sb_2O_3$ , which was then compressed to a hard solid using a hydraulic laboratory press. Antimony oxide was chosen for several reasons:

- It is the species with which a proof of concept had been established.,
- It is not overly toxic in the event of an accidental leak or contamination as the system was debugged, and
- Antimony is relevant as a fugitive emission from incinerators and other industries.

Nitrogen is flowed through the dust feeder to entrain the Oxide particles. A calibrated rotameter is used to control the $N_2$ flow. The Wright dust feeder produces entrained particles in a gas flow by passing the gas over the hard-pressed solid block as a rotating mechanical knife edge scrapes the block. By varying the scraper rotation rate, the user sets the entrained particle concentration since the preferred gas rate is fixed. Since these flows are greater than desired for the reactor, portion of the dust-laden $N_2$ is bypassed to

vent after dropping particles in a crude flask separator. Metal Oxide particles entrained in nitrogen are then passed through the calibrated venturi meter and then introduced to the Preheater. Reagent HCl gas (95 mole% nitrogen and 5% HCl) is also introduced through a calibrated rotameter just before the preheater.

The preheater temperature controller is set for 150 C. After the preheater, the flow passes into the reactor. The furnace controllers were set for 300 C for the initial runs, with later runs performed at 400C.

Product metal chloride vapors, unreacted metal oxide particles and HCl (with $N_2$) exit the reactor and are bubbled through two glass bubblers in series, each containing standard NaOH solution of known molarity (typically 0.0002M). The unreacted HCl is neutralized by NaOH until the end point is reached. The time of titration is noted using an electronic stopwatch.

HCl conversion is calculated using the molarity of NaOH solution, inlet feed flowrate of HCl to the reactor and titration time.

Different sets of data were collected in the following way:

- Keeping the reactor residence time and dust feeder rate constant and varying the HCl rate.
- Keeping dust feeder rate and HCl rate constant and varying the residence time.
- Keeping residence time and HCl rate constant and varying the rate of the dust feeder.

Tables 2.1, 2.3 and 2.5 give the molar flow rates of HCl at the inlet and outlet based on flows and titration time respectively.

Experimental uncertainties were present through:

- Inaccuracies in recording the titration time
- Slight differences in the concentration of standard NaOH solution
- Fluctuations and drops in the flows of HCl and $N_2$
- Loss of HCl in the vent after the bubblers
- Accumulation of dust particles in the reactor tube or outlet line

Although the last four reasons can cause significant variations, the NaOH solutions were prepared and standardized very carefully. Gas flows were controlled efficiently. The remaining HCl exiting the reactor is almost totally consumed in the first bubbler as the end point is never reached in the second bubbler. Finally the $N_2$ flow is high enough that the accumulation of particles (i.e. settling) does not appear to be significant. The only significant factor, which gives uncertainty and deviation in the results, is the imprecision in recording the titration time. As the NaOH solution is very dilute and since the molar rate of gaseous HCl is low, a difference of a few seconds in measured titration time can yield considerable uncertainties in the molar rates at the outlet of the reactor. These uncertainties must be accounted for in the conversion measured as a function of HCl rate. To take into account this uncertainty, error (uncertainty) bars have been put on the curves for HCl conversion versus HCl rate. These error bars show that the conversions are known to with about $\pm$ 4 percentage points.

Figs.2.2a, 2.3a, and 2.4a indicate that there is a clear difference in the titration times with and without flowing dust particles through the reactor. This shows that there is definite chemical conversion. The titration time decreases with increasing HCl rate because more HCl is available to neutralize the NaOH solution.

Figures 2.2b and 2.3b show that there is little, if any, effect on conversion as a function of molar flow rates of HCl at a constant dust rate. Table 2.6 and Fig.2.4b indicate that slightly more conversion is achieved at a higher dust rate, keeping all other conditions same. This is because more HCl is consumed when more dust particles are flowing through the reactor. In addition, there appears to be an improved trend in Fig. 2.4b. Tables 2.7, 2.8 and 2.9 gives the HCl conversion as a function of dust rate for runs 13-22 for three different HCl rates. Figs.2.6, 2.7 and 2.8 show HCl conversion increases by increasing the particle flow rate through the reactor. This is again because more HCl is consumed reacting at the higher dust rate. But the monotonic trend in conversion was fairly independent of HCl rate as seen earlier.

Runs 23-25 have been performed at a furnace set point 400C. More precision in the titration times. The conversion increases substantially compared to the comparable runs at furnace set point 300C (e.g. Fig.2.2b). However as seen earlier, the conversion is effectively independent of HCl rate.

***Keeping Residence time and dust rate constant and varying HCl rate at 300C***

Molarity of NaOH Solution = $1.8 * 10^{-4}$ M (250 ml solution taken in bubbler)

Flow rate of N2 = 0.2 SCFM

Pre-heater temperature controller set point = 150 C

Reactor temperature controller set point = 300 C

Effluent temperature controller set point = 100 C

Dust rate = 0.0206 g/min (0.43 rpm)

**Table 2.1** Concentration of HCl at the inlet and outlet of reactor for runs 1-4

| Run # | Conc. of HCl at inlet Based on Flows(mol/ml) | Conc. of HCl at outlet Based on Titration(mol/ml) | Δ |
|---|---|---|---|
| 1 | $1.8 * 10^{-9}$ | $1.403 * 10^{-9}$ | $3.97 * 10^{-10}$ |
| 2 | $1.416 * 10^{-9}$ | $1.08 * 10^{-9}$ | $3.36 * 10^{-10}$ |
| 3 | $1.063 * 10^{-9}$ | $8.66 * 10^{-10}$ | $1.97 * 10^{-10}$ |
| 4 | $7.08 * 10^{-10}$ | $5.40 * 10^{-10}$ | $1.68 * 10^{-10}$ |

**Table 2.2** Titration time and HCl conversion as a function of HCl rate for runs 1-4

| Run # | HCl rate (ml/min) | Titration time without particles | Titration time with particles (min) | HCl conversion % |
|---|---|---|---|---|
| 1 | 4.62 | 5.66 | 7.33 | 40.4 |
| 2 | 3.61 | 7.33 | 8.66 | 35.55 |
| 3 | 2.7 | 9.16 | 12 | 37.77 |
| 4 | 1.8 | 14.66 | 19.50 | 42.56 |
| Average | | | | 39.07 |

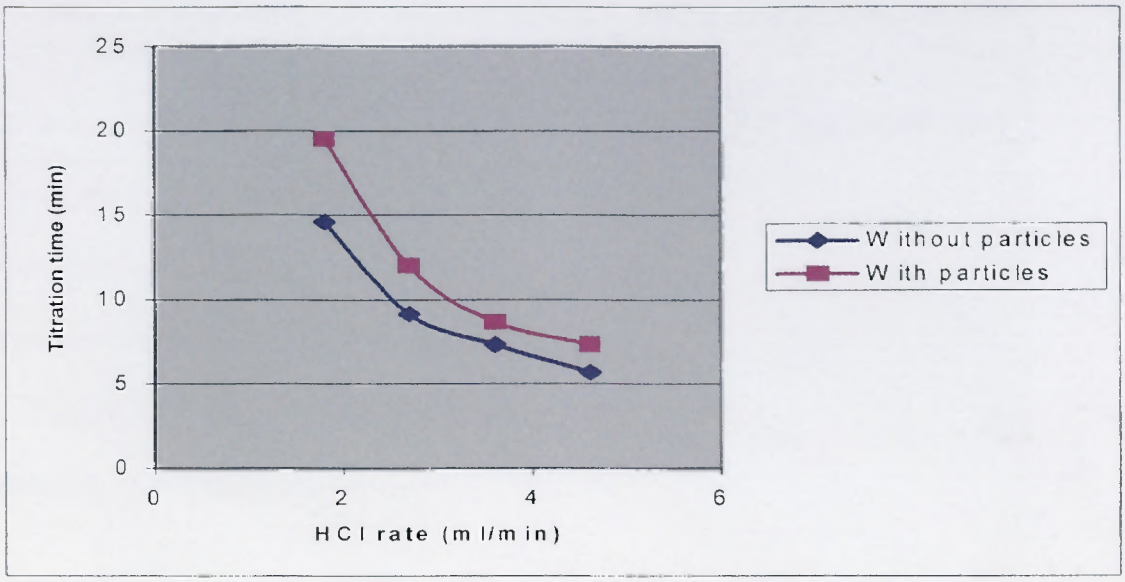


**Figure 2.2a** HCl Rate Versus Titration Time for runs 1-4

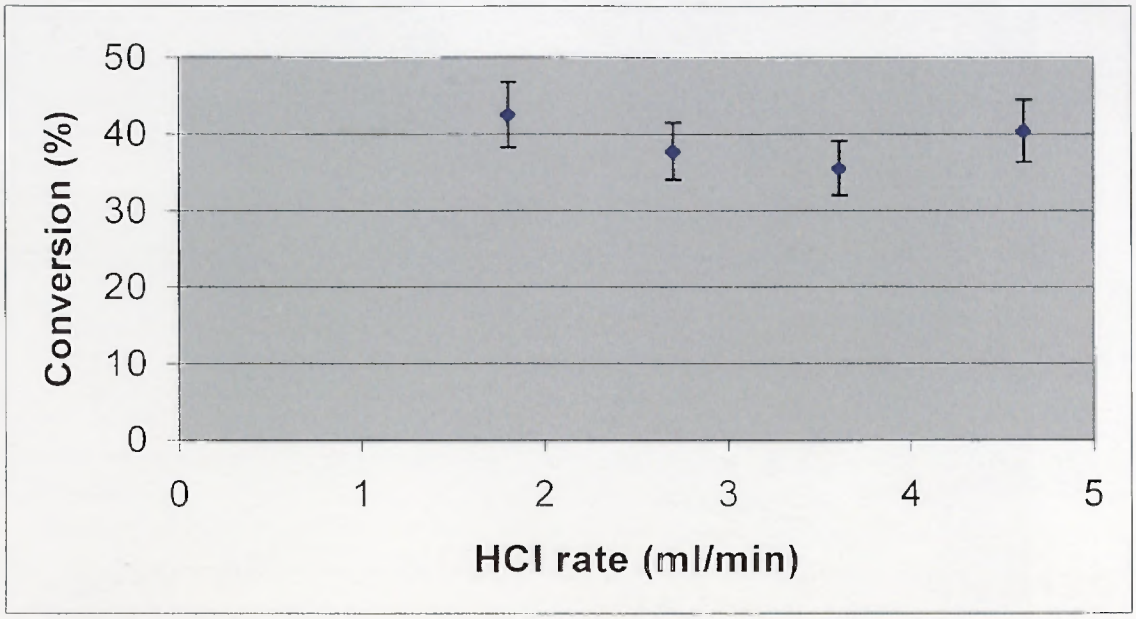


**Figure 2.2b** HCl Rate Versus Conversion for runs 1-4

***Keeping Residence time and dust rate constant and varying HCl rate at 300C (At low residence time)***

Molarity of NaOH Solution = $1.8 * 10^{-4}$ M (250 ml solution taken in bubbler)

Flow rate of N2 = 0.14 SCFM

Pre-heater temperature controller set point = 150 C

Reactor temperature controller set point = 300 C

Effluent temperature controller set point = 100 C

Dust rate = 0.0206 g/min (0.43 rpm)

**Table 2.3** Concentration of HCl at the inlet and outlet of reactor for runs 5-8

| Run # | Conc. of HCl at inlet Based on Flows(mol/ml) | Conc. of HCl at outlet Based on Titration(mol/ml) | Δ |
|---|---|---|---|
| 5 | $2.42 * 10^{-9}$ | $1.7 * 10^{-9}$ | $7.2 * 10^{-10}$ |
| 6 | $1.888 * 10^{-9}$ | $1.51 * 10^{-9}$ | $3.7 * 10^{-10}$ |
| 7 | $1.42 * 10^{-9}$ | $1.13 * 10^{-9}$ | $2.9 * 10^{-10}$ |
| 8 | $9.44 * 10^{-10}$ | $6.82 * 10^{-10}$ | $2.62 * 10^{-10}$ |

**Table 2.4** Titration time and HCl conversion as a function of HCl rate for runs 5-8

| Run # | HCl rate (ml/min) | Titration time without particles | Titration time with particles (min) | HCl conversion % |
|---|---|---|---|---|
| 5 | 4.62 | 6.16 | 7.66 | 43.8 |
| 6 | 3.61 | 7 | 8.33 | 32.98 |
| 7 | 2.7 | 9.33 | 11.66 | 36 |
| 8 | 1.8 | 15.50 | 19.50 | 42.56 |
| Average | | | | 38.83 |

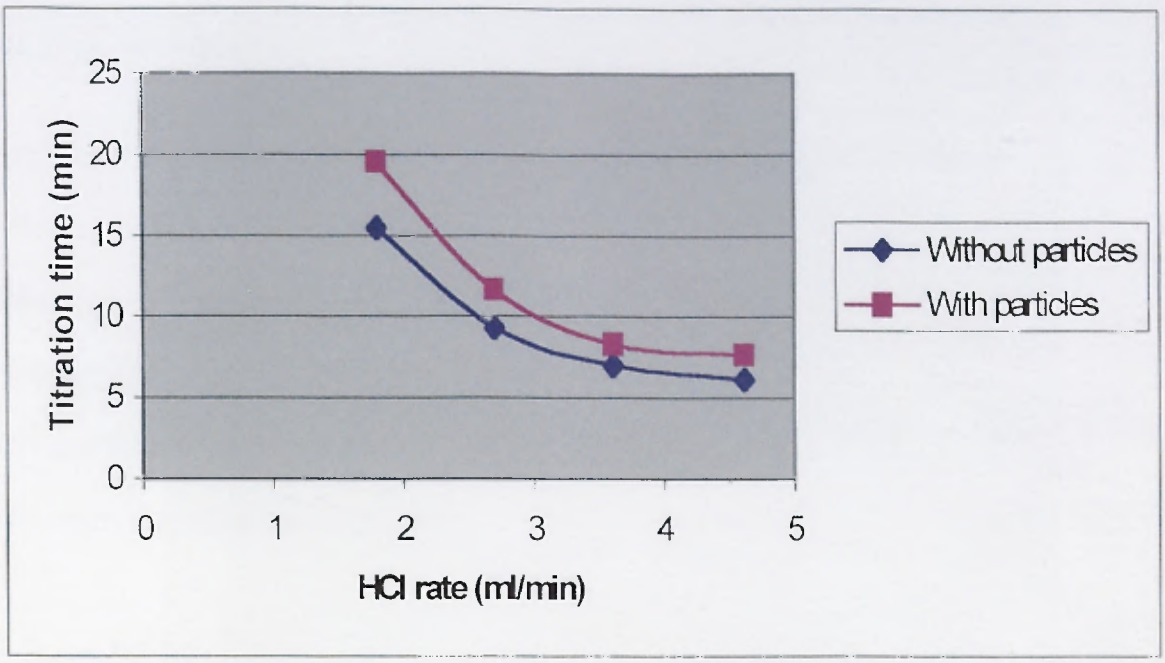


**Figure 2.3a** HCl Rate Versus Titration Time for runs 5-8

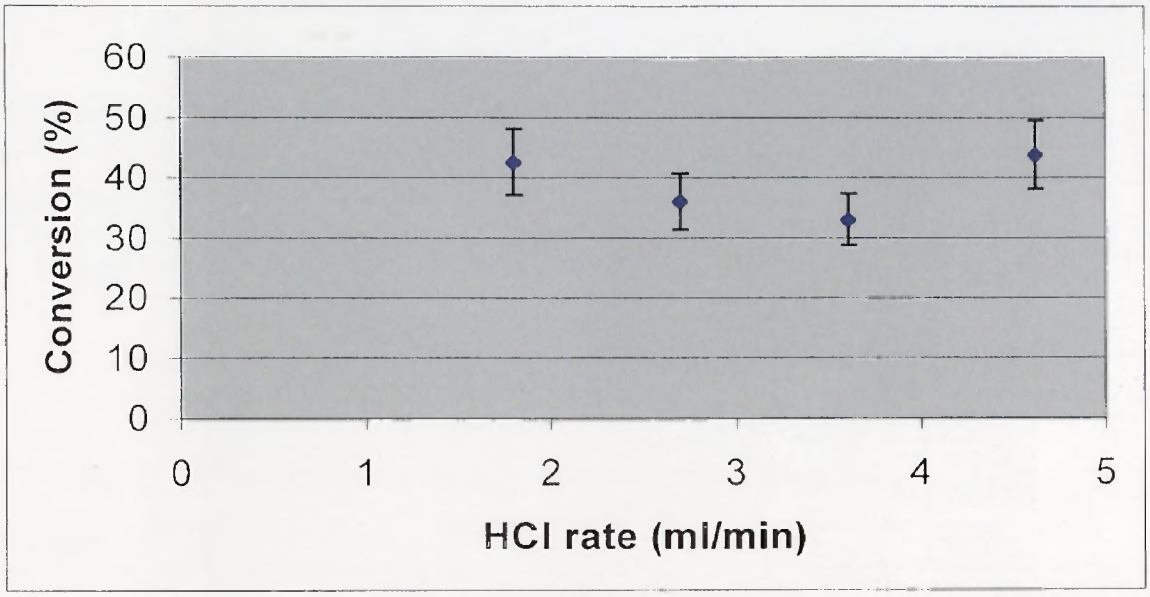


**Figure 2.3b** HCl Rate Versus Conversion for runs 5-8

***Keeping Residence time and dust rate constant and varying HCl rate at 300C (At high dust rate)***

Molarity of NaOH Solution $=1.2 * 10^{-4}$ M (250 ml solution taken in bubbler)

Flow rate of N2 = 0.14 SCFM

Pre-heater temperature controller set point = 150 C

Reactor temperature controller set point = 300 C

Effluent temperature controller set point = 100 C

Dust rate = 0.026 g/min (0.55 rpm)

**Table 2.5** Concentration of HCl at the inlet and outlet of reactor for runs 9-12

| Run # | Conc. of HCl at inlet Based on Flows(mol/ml) | Conc. of HCl at outlet Based on Titration(mol/ml) | Δ |
|---|---|---|---|
| 9 | $3.08 * 10^{-9}$ | $2.49 * 10^{-9}$ | $5.9 * 10^{-10}$ |
| 10 | $2.42 * 10^{-9}$ | $1.69 * 10^{-9}$ | $7.3 * 10^{-10}$ |
| 11 | $1.88 * 10^{-9}$ | $1.32 * 10^{-9}$ | $5.6 * 10^{-10}$ |
| 12 | $1.42 * 10^{-9}$ | $1.05 * 10^{-9}$ | $3.7 * 10^{-10}$ |

**Table 2.6** Titration time and HCl conversion as a function of HCl rate for runs 9-12

| Run # | HCl rate (ml/min) | Titration time without particles | Titration time with particles (min) | HCl conversion % |
|---|---|---|---|---|
| 9 | 5.87 | 2.833 | 4.33 | 47.11 |
| 10 | 4.62 | 4.16 | 5.50 | 47.1 |
| 11 | 3.61 | 5.33 | 6.50 | 42.72 |
| 12 | 2.7 | 6.66 | 8 | 37.78 |
| Average | | | | 43.67 |

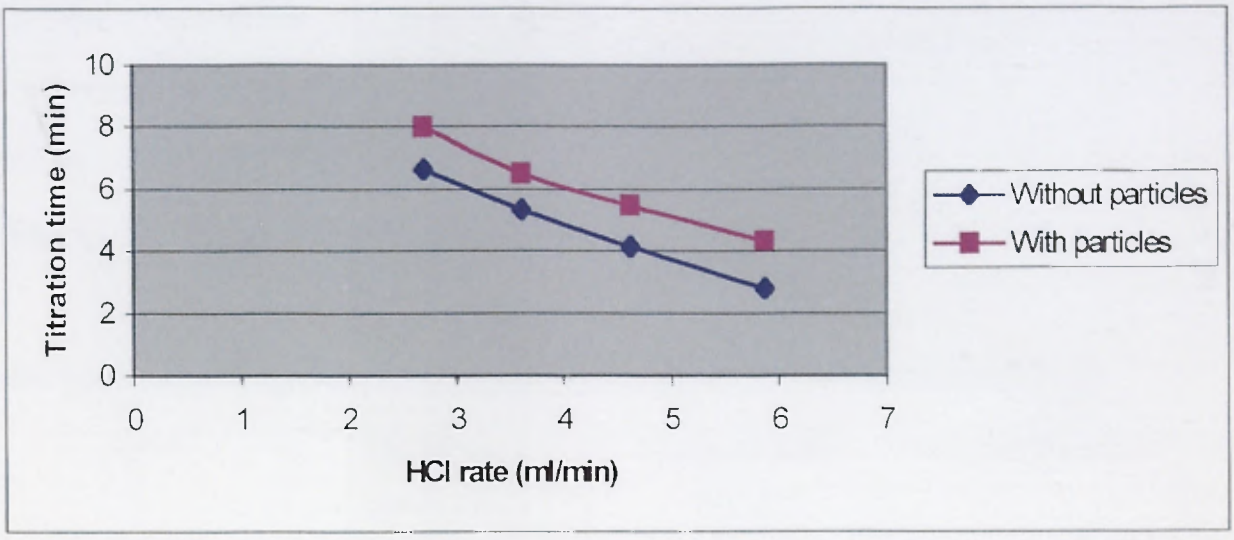


**Figure 2.4a** HCl Rate Versus Titration Time for runs 9-12

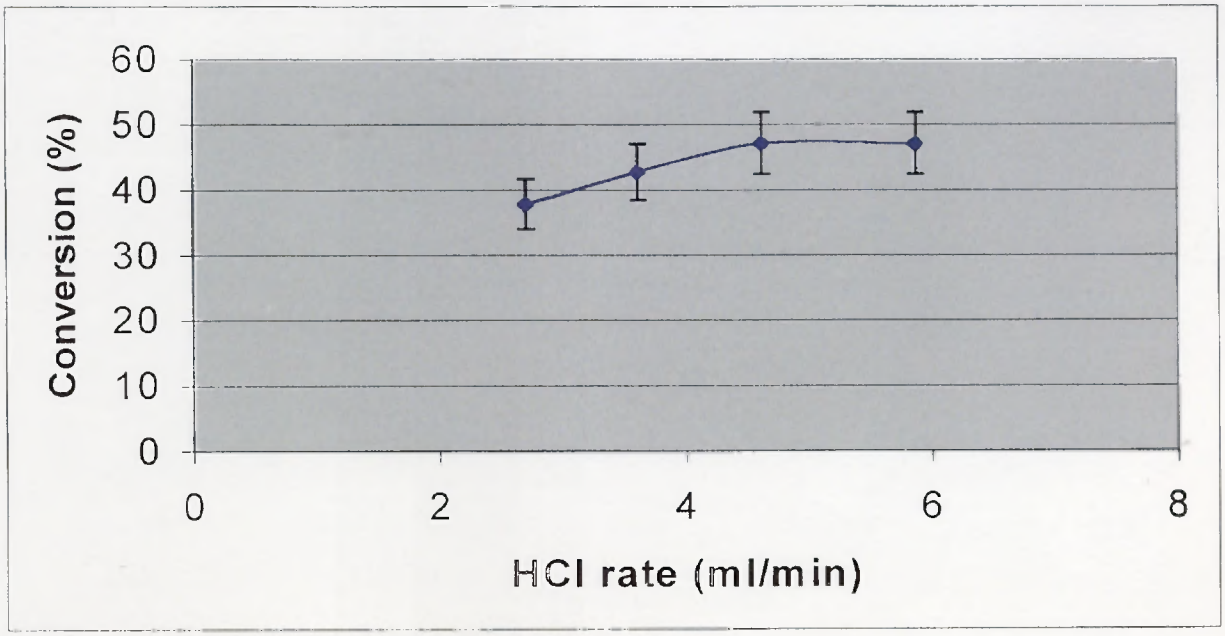


**Figure 2.4b** HCl Rate Versus Conversion for runs 9-12

***Keeping HCl rate constant and varying Oxide rate at 300C***

HCl rate = 4.62 ml/min

Molarity of NaOH solution =2 * $10^{-4}$ M

N2 flow rate =0.15 SCFM

Titration time without particles flow = 6 min

**Table 2.7** Titration time and HCl conversion as a function of dust rate for runs 13-15

| Run # | Dust rate (gm/min) | Titration time (min) | HCl conversion % |
|---|---|---|---|
| 13 | 0.01 (0.20 rpm) | 7.33 | 33.85 |
| 14 | 0.0153 (0.30 rpm) | 8.16 | 40.58 |
| 15 | 0.0256 (0.50 rpm) | 8.33 | 41.79 |

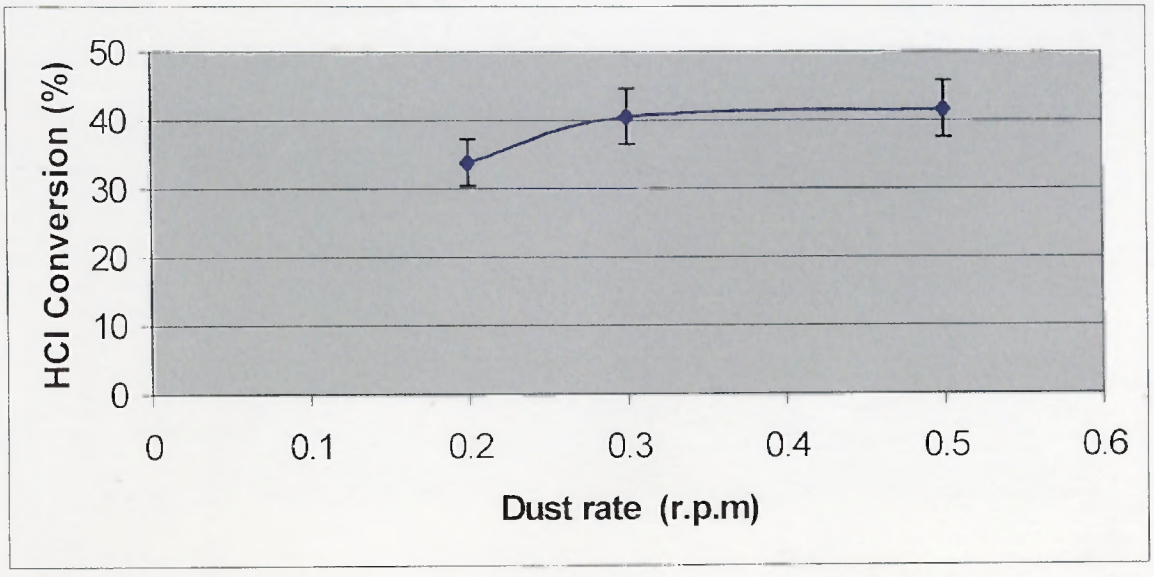


**Figure 2.6** Dust rate versus conversion for runs 13-15

***Keeping HCl rate constant and varying Oxide rate***

HCl rate =2.7 ml/min

Molarity of NaOH solution =1 * $10^{-4}$ M

N2 flow rate =0.15 SCFM

Titration time without particles flow = 5.833 min

**Table 2.8** Titration time and HCl conversion as a function of dust rate for runs 16-19

| Run # | Dust rate (gm/min) | Titration time (min) | HCl conversion % |
|---|---|---|---|
| 16 | 0.01 (0.20 rpm) | 6 | 30.86 |
| 17 | 0.0153 (0.325 rpm) | 6.66 | 37.70 |
| 18 | 0.021 (0.450 rpm) | 8.16 | 49.17 |
| 19 | 0.0256 (0.55 rpm) | 8.33 | 50.20 |

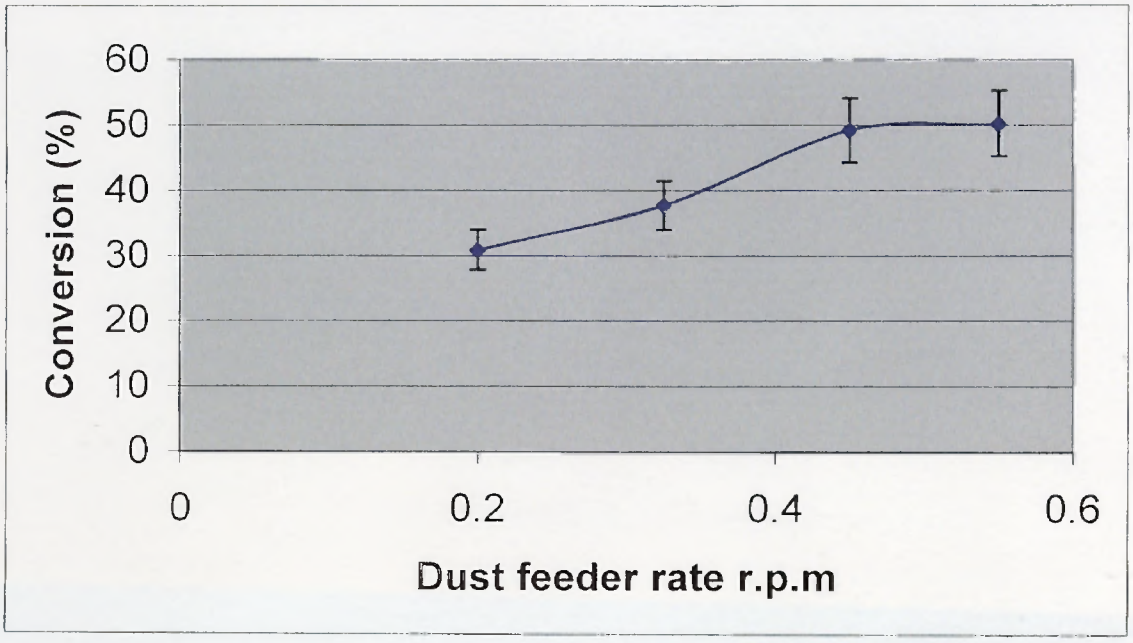


**Figure 2.7** Dust rate versus conversion for runs 16-19

*Keeping HCl rate constant and varying Oxide rate at 300C*

HCl rate =5.87 ml/min

Molarity of NaOH solution =$1.2 * 10^{-4}$ M

N2 flow rate =0.15 SCFM

Titration time without particles flow =2.833 min

**Table 2.9** Titration time and HCl conversion as a function of dust rate for runs 20-22

| Run # | Dust rate (gm/min) | Titration time (min) | HCl conversion % |
|---|---|---|---|
| 20 | 0.0153 (0.30 rpm) | 3.5 | 34.58 |
| 21 | 0.020 (0.405 rpm) | 4 | 42.76 |
| 22 | 0.0256 (0.55 rpm) | 4.33 | 47.12 |

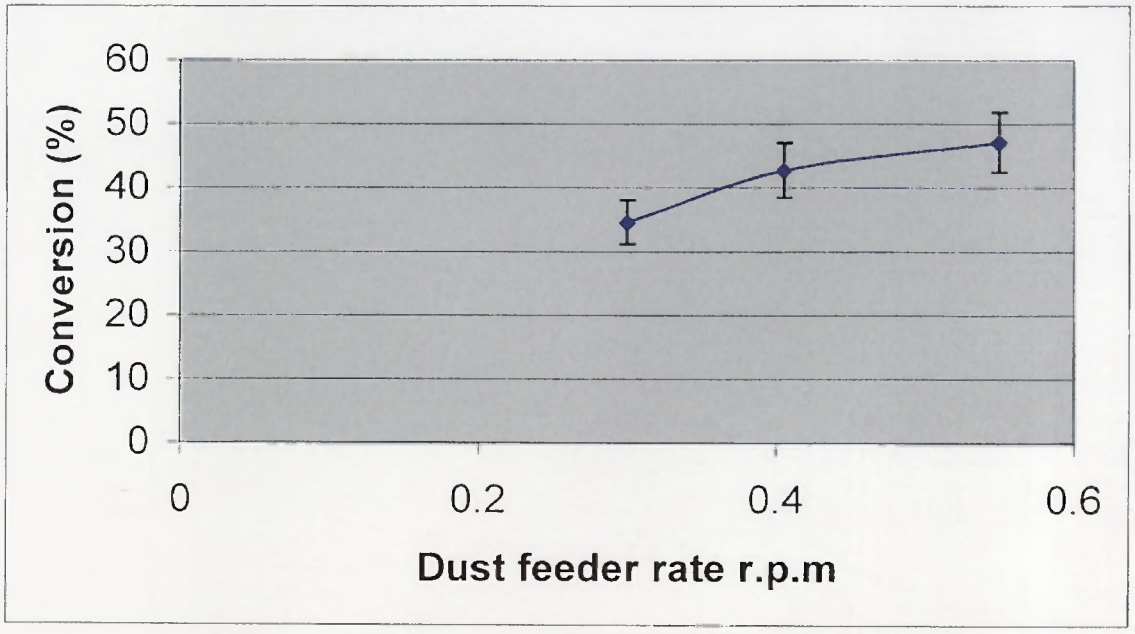


**Figure 2.8** Dust rate versus conversion for runs 20-22

***Keeping Residence time and dust rate constant and varying HCl rate at 400C***

Molarity of NaOH Solution = $1.5 * 10^{-4}$ M (250 ml solution taken in bubbler)

Flow rate of N2 = 0.2 SCFM

Pre-heater temperature controller set point = 150 C

Reactor temperature controller set point = 400 C

Effluent temperature controller set point = 100 C

Dust feeder rate = 0.0206 g/min (0.40 rpm)

**Table 2.10** Concentration of HCl at the inlet and outlet of reactor for runs 23-25

| Run # | Conc. of HCl at inlet Based on Flows(mol/ml) | Conc. of HCl at outlet Based on Titration(mol/ml) | Δ |
|---|---|---|---|
| 23 | $2.3 * 10^{-9}$ | $1.420 * 10^{-9}$ | $8.8 * 10^{-10}$ |
| 24 | $1.80 * 10^{-9}$ | $1.07 * 10^{-9}$ | $7.3 * 10^{-10}$ |
| 25 | $1.42 * 10^{-9}$ | $7.97 * 10^{-10}$ | $6.23 * 10^{-10}$ |

**Table 2.11** Titration time and HCl conversion as a function of HCl rate for runs 23-25

| Run # | HCl rate (ml/min) | Titration time without particles | Titration time with particles (min) | HCl conversion % |
|---|---|---|---|---|
| 23 | 5.86 | 4.66 | 6.83 | 60 |
| 24 | 4.62 | 6.16 | 9.30 | 61.6 |
| 25 | 3.61 | 8.30 | 11.16 | 58.2 |
| Average | | | | 59.93 |

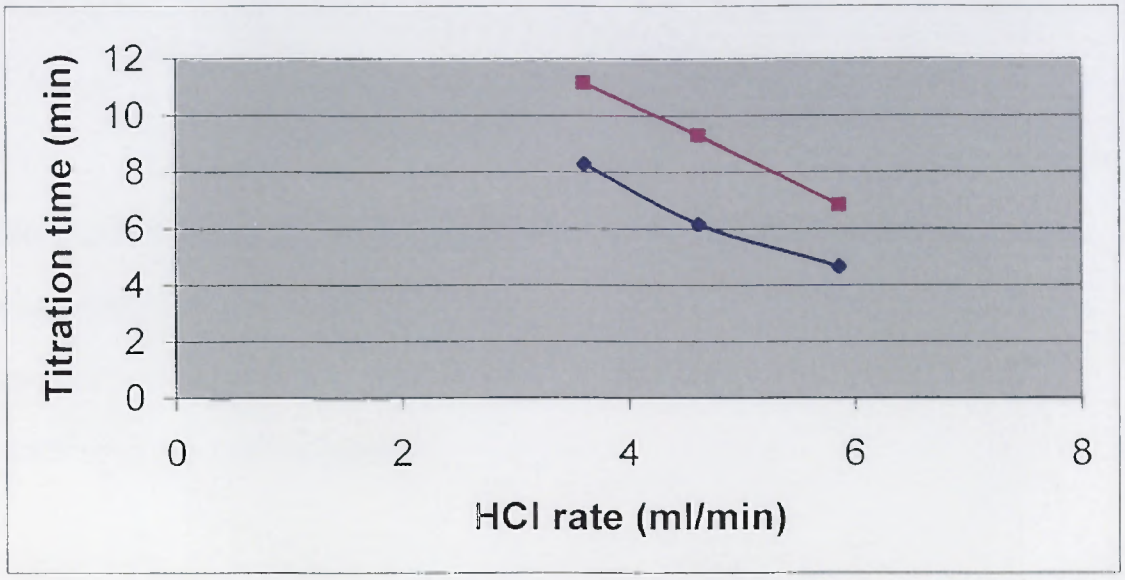


**Figure 2.9a** HCl rate versus Titration Time for runs 23-25

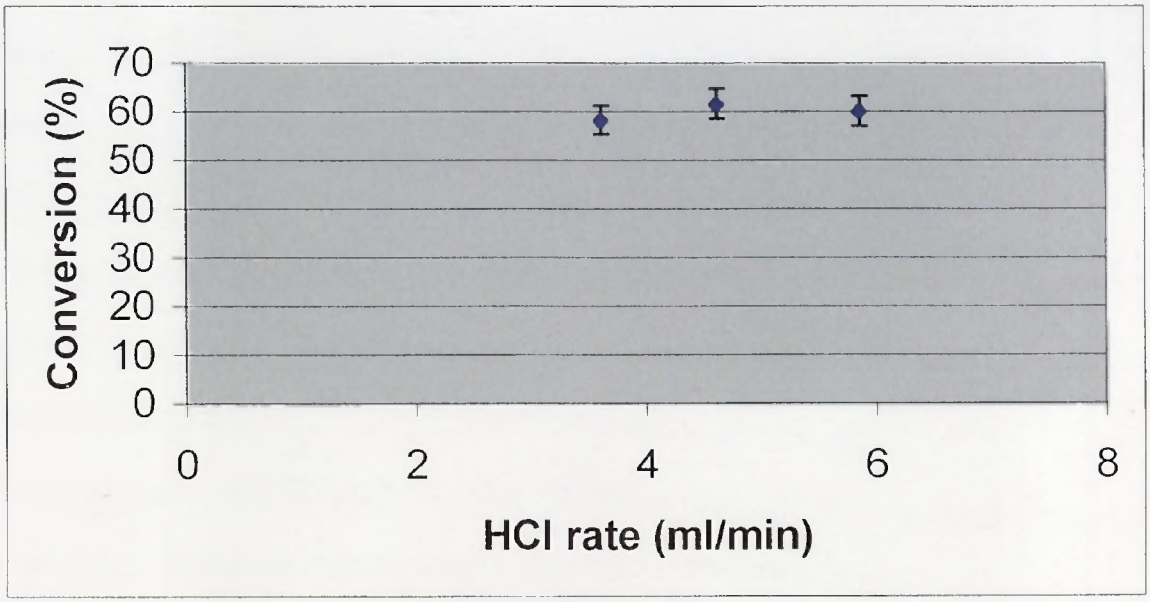


**Figure 2.9b** HCl rate Versus Conversion for runs 23-25

# CHAPTER 3

## THE KINETICS OF THE GAS-SOLID REACTION BETWEEN $Sb_2O_3$ AND HCL

The smallest representative unit of a gas-solid reaction system is the interaction of a single particle with a moving gas stream. The study of single-particle systems can be generalized to the more complex multiparticle assemblies. The reaction of solid Antimony oxide with HCl gas is:

$$6HCl\,(g) + Sb_2O_3\,(s) \rightarrow 2SbCl_3\,(g) + 3H_2O\,(g) \qquad (2.1)$$

### 3.1 Shrinking Core Model with no Ash Layer

The reaction between $Sb_2O_3$ and gaseous HCl likely follows the shrinking core model [3], where the particle shrinks during reaction, no ash layer forms, and the particle finally disappears. This process is illustrated in Figure 3.1. For a reaction of this kind, the following three steps have been visualized to occur in succession [3].

**Step1** Diffusion of reactant A from the main body of the gas through the gas film to the surface of the solid.

**Step2** Adsorption of reactant A onto solid surface

**Step3** Surface Reaction between gaseous reactant A and solid.

**Step4** Desorption of gaseous products from solid surface

**Step5** Diffusion of gaseous products from the surface of the solid through the gas film into the main body of the gas.

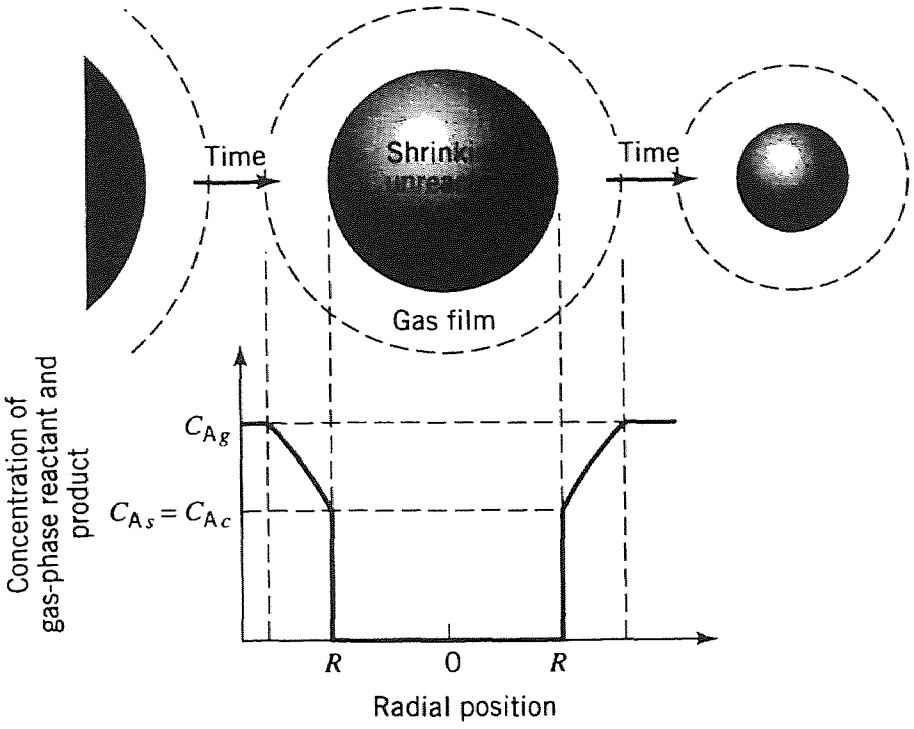


**Figure 3.1** Representation of concentration of reactants and products for the reaction between a shrinking $Sb_2O_3$ particle and gaseous HCl.

### 3.2 Mass Transfer between Single Particles of $Sb_2O_3$ and a moving HCl Gas Stream:

The rate at which gaseous reactants are transferred through the boundary layer from the bulk gas to the outer surface of the solid or the rate at which gaseous products are removed from the outer surface to the bulk can play an important role in determining the overall rate of reaction.

Let A denotes the gaseous transferred reactant HCl, the concentration of which is then designated by $C_{AS}$ and $C_{A0}$ at the solid surface and in the bulk of the gas stream, respectively. Then the rate at which A is being transferred across the boundary layer per unit solid surface area is given by

$$N_A = h_D (C_{AS} - C_{A0})$$

where $h_D$ is the mass transfer coefficient, which is defined by this equation. The concentration may be expressed as either moles per unit volume or mass per unit volume and the flux of the transferred species, $N_A$, is given in the corresponding units. But in this reaction system the temperature is probably low enough that mass transfer through gas film is not controlling.

### 3.3 Langmuir Hinshelwood Rate Constant for the Reaction between $Sb_2O_3$ and HCl

The reaction between Antimony oxide and HCl is

$$6\,HCl(g) + Sb_2O_3(s) \rightarrow 2\,SbCl_3(g) + 3\,H_2O(g)$$

$$HCl(g) + \frac{1}{6}Sb_2O_3(s) \rightarrow \frac{1}{3}SbCl_3(g) + \frac{1}{2}H_2O(g)$$

$$A(g) + \frac{1}{6}B(s) \rightarrow \frac{1}{3}C(g) + \frac{1}{2}D(g)$$

The reaction process will involve the adsorption of the reactant gas A on the surface of solid B to form a surface complex X*, which transforms to another surface complex Y*, which then desorbs to give the gaseous product C.

$$A(g) + S \Leftrightarrow X^{*} \quad (adsorption) \qquad (3.2)$$

$$X^{*} \Leftrightarrow Y^{*} + D(g) \quad (reaction) \qquad (3.3)$$

$$Y^{*} \Leftrightarrow C + S \quad (desorption) \qquad (3.4)$$

Where S designates the bare solid surface site that is available to both A and C, and the reaction involves complete gasification of solid. The product D is assumed to leave directly (i.e. without desorption) according to an Eley-Rideal step.

The net rates of adsorption of A and desorption of C may be written as:

Net rate of adsorption of A = Rate of adsorption of A – Rate of desorption of A

$$r_1 = k_1 P_A \theta_S - k_{-1} \theta_x^* \qquad (3.4)$$

Where $k_{1,-1}$ = Rate constants for adsorption and desorption of A respectively

$P_A$ = Partial pressure of A

$\theta_S$ = Fraction of vacant sites (i.e. available for reaction)

$\theta_X^*$ = Fraction of sites occupied by surface complex X*

Net rate of desorption of C = Rate of desorption of C - Rate of adsorption of C

$$r_3 = k_{-3} \theta_Y^* - k_3 P_c \theta_s \qquad (3.5)$$

Where $k_{3,-3}$ = Rate constants for adsorption and desorption of C respectively

$P_C$ = Partial pressure of C

$\theta_Y^*$ = Fraction of sites occupied by surface complex Y*

Over all balance on the sites is:

$$\theta_S + \theta_X^* + \theta_Y^* = 1$$

***Surface Reaction Controlling:***

If the surface reaction is the slow step and hence controls the overall rate, the adsorption and desorption steps will be in fast equilibrium; i.e.,

$$\frac{r_1}{k_1} \approx \frac{r_3}{k_{-3}} \approx 0$$

$$(\theta_X^*)_{eq} = \left(\frac{k_1}{k_{-1}}\right) P_A \theta_S = K_1 P_A \theta_S \qquad (3.6)$$

$$(\theta_Y^*)_{eq} = \left(\frac{k_3}{k_{-3}}\right) P_C \theta_S = K_3 P_C \theta_S \qquad (3.7)$$

Where $k_1/k_{-1}=K_1$ and $k_3/k_{-3}= K_3$ are adsorption equilibrium constants.

The net forward rate of surface reaction is then given by:

$$r_2 = k_2 \theta_X^* - k_{-2} \theta_Y^* P_D \qquad (3.8)$$

Substituting the values of $\theta_x^*$ and $\theta_Y^*$

$$r_2 = k_2 K_1 P_A \theta_S - k_{-2} K_3 P_C P_D \theta_S \qquad (3.9)$$

Substituting the expression for $\theta_X^*$ and $\theta_Y^*$ into the site balance provides an expression for the fraction of vacant sites:

$$\theta_S = \frac{1}{1 + K_1 P_A + K_3 P_C}$$

At steady state , the overall net forward rate will be:

$$r = r_2 = \frac{k_2 K_1 P_A - k_{-2} K_3 P_C P_D}{1 + K_1 P_A + K_3 P_C} \qquad (3.10)$$

$$r = \frac{k_2 K_1 \left( P_A - \frac{K_3}{K_1 K_2} P_C P_D \right)}{1 + K_1 P_A + K_3 P_C} \qquad (3.11)$$

Where $K_2 = k_2 / k_{-2}$ = Equilibrium constant for the reaction step.

The three steps of adsorption, reaction and desorption occur in series; hence, the product of their equilibrium constants is the $K_{eq}$ for the entire mechanism.

$$\frac{K_1 K_S}{K_3} = K_{eq}$$

If $K_{eq}$ is large (favorable), then

$$r \approx \frac{k_2 K_1 P_A}{1 + K_1 P_A + K_3 P_C} \qquad (3.12)$$

There is another, implicit assumption here. The oxide particles are shrinking. It is assumed that the time scale for diffusion (external), adsorption/desorption and surface reaction are relatively short compared to the time scale for complete particle shrinkage. This allows us to assume an approximate steady state regarding the size of the particle. Equation 3.12 becomes the assumed working rate expression for the experiment in this study.

# CHAPTER 4

# REACTOR CHARACTERIZATION

## 4.1. Curve Fit of Experimental Temperature Profile

Axial temperature profile measurements revealed that the reactor is, infect, not isothermal and temperature is a function of axial position Z. The experimental Temperature Profiles are the curves fitted as shown in Figure 4.1 and 4.2 in order to obtain a polynomial expression for T that will be used for mathematical modeling to calculate the kinetic parameters. The curve fits of Axial Temperature profiles are:

At reactor furnace set point temperature of 300 C:

$$T = -0.0309Z^2 + 4.634Z + 398.87$$

At reactor furnace set point temperature of 400 C:

$$T = -0.0948Z^2 + 9.6989Z + 436.3$$

Where T has units of Kelvin and Z has units of cm.The reactor length is 66cm, and the figures 4.1 and 4.2 give the temperatures as a function of distance from the inlet to the end of the reactor.

## 4.2. Profile of Reynolds Number

As part of the reactor characterization, the Reynolds number must be determined. Reynolds number is a dimensionless group that could be used to predict the nature of the flow (i.e. laminar, turbulent)

$$N_{Re} = \frac{D\ G}{\mu}$$

Where D is the pipe diameter and G is the mass velocity. μ is the fluid viscosity and is a function of temperature

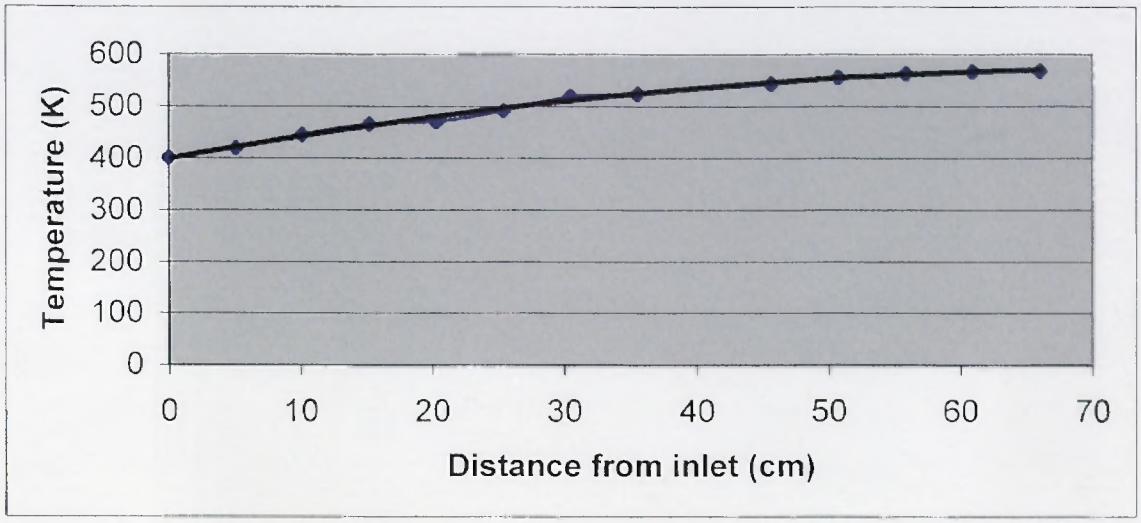


**Figure 4.1** Temperature profile at 300C

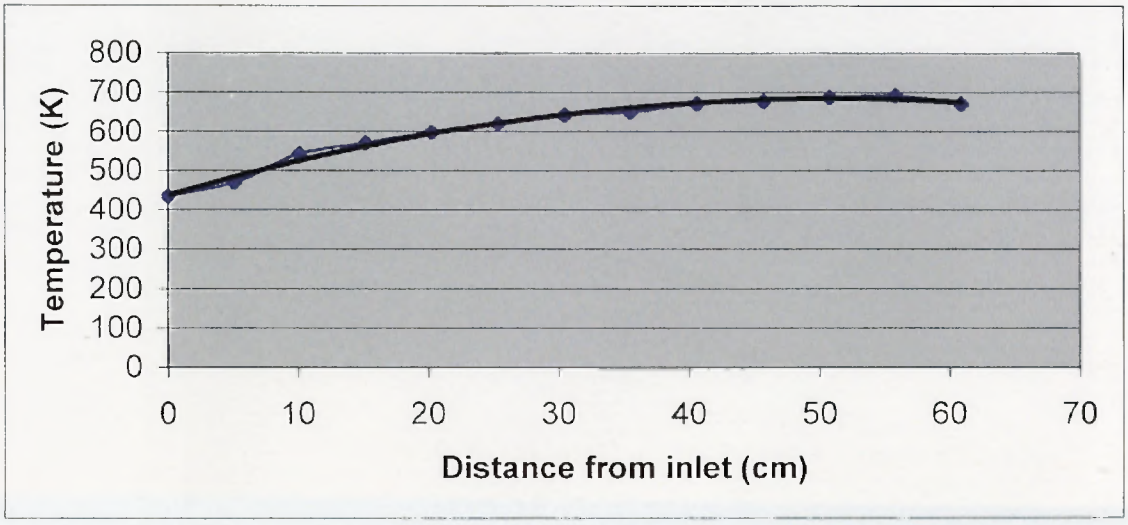


**Figure 4.2** Temperature profile at 400C

Flow is considered laminar for Reynolds number below 2100; and for Reynolds number of more than 4000 the flow is fully turbulent [5].

Tables 4.1 and 4.2, and figure 4.3 illustrate the variation in Reynolds number through the tube.

**Table 4.1** Temperature and Reynolds number profile at furnace set point 300C

| **Distance from the inlet (cm)** | **Temperature K** | **Reynolds Number** |
|---|---|---|
| 0 | 401 | 8078.088 |
| 5.08 | 419 | 7899.961 |
| 10.16 | 445 | 7404.886 |
| 15.24 | 466 | 7165.264 |
| 20.32 | 471 | 7165.264 |
| 25.4 | 492 | 6709.049 |
| 30.48 | 520 | 6585.721 |
| 35.56 | 525 | 6462.762 |
| 45.72 | 544 | 6236.087 |
| 50.8 | 556 | 6128.348 |
| 55.88 | 563 | 6129.396 |
| 60.96 | 567 | 6024.774 |
| 66.04 | 568 | 6026.295 |

**Table 4.2** Temperature and Reynolds number profile at 400C

| Distance from the inlet (cm) | Temperature K | Reynolds Number |
|---|---|---|
| 0 | 434 | 7729.519 |
| 5.08 | 469 | 7165.264 |
| 10.16 | 541 | 6230.665 |
| 15.24 | 571 | 6026.295 |
| 20.32 | 597 | 5921.706 |
| 25.4 | 620 | 5732.211 |
| 30.48 | 642 | 5554.468 |
| 35.56 | 651 | 5554.468 |
| 40.64 | 671 | 5469.667 |
| 45.72 | 678 | 5469.667 |
| 50.8 | 688 | 5387.417 |
| 55.88 | 692 | 5387.417 |
| 60.96 | 671 | 5469.667 |

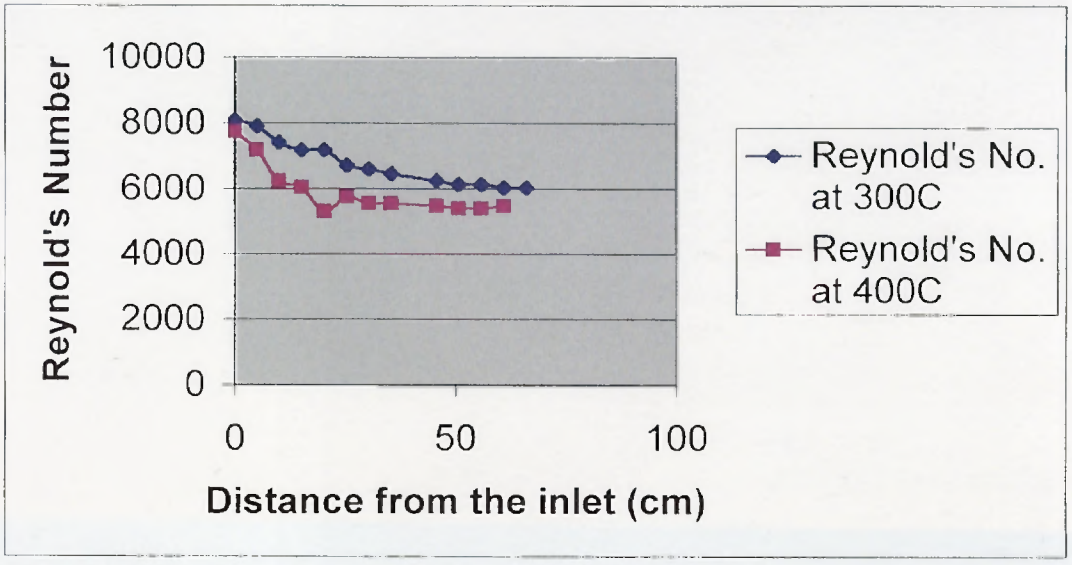


**Figure 4.3** Reynolds number profile at 300C and 400C

### 4.3 Key Assumptions

As the Reynolds number varies between 8000 and 6000 at furnace set point 300C and from 7729 to 5400 at furnace set point 400C through the reactor length, therefore the fluid flow is very much turbulent. So this assumption is justified that there is little or no radial variation in concentration. Hence the reactor is referred to as a Plug-flow reactor (PFR). The reactants are continually consumed as they flow down the length of the reactor and the concentration varies continuously in the axial direction through the reactor [2].

The small diameter of the reactor quartz tube (1/4 inches) facilitates the assumption of a lack of a significant radial temperature dependence.

The model for a PFR will be developed. It will then be combined with the kinetic rate expression to establish a performance equation for correlation of the experimental data.

# CHAPTER # 5

## MATHEMATICAL MODELING TO CALCULATE THE KINETIC PARAMETERS FOR A REACTION BETWEEN $Sb_2O_3$ AND HCl

There is a need to develop a model in order to estimate Kinetic parameters for the gas-solid reaction between $Sb_2O_3$ and HCl. To develop this model we will do a differential mole balance in a PFR. We will then use the postulated rate law from chapter 3 and the measured temperature profile (chapter 4).

The model reaction is:

$$A\ (g) + \frac{1}{6} B\ (s) \rightarrow \frac{1}{3} C\ (g) + \frac{1}{2} D\ (g)$$

In the PFR, the reactants are continually consumed as they flow down the length of the reactor. In modeling the PFR, we assume that the concentration varies continuously in the axial direction through the reactor. Consequently, the reaction rate, which is a function of concentration and temperature, will also vary axially. The general plug flow reactor differential mole balance is given by :

$$F_A\big|_V - F_A\big|_{V+\Delta V} + r_A \Delta V = 0 \qquad (5.1)$$

$$-\Delta F_A + r_A \Delta V = 0 \qquad (5.2)$$

Where $F_A$ is the molar flow rate of reactant A. The volume $\Delta V$ is the product of the cross-sectional area $A_C$ of the reactor and the reactor length $\Delta Z$.

$$-dF_A + r_A A_C dZ = 0 \qquad (5.3)$$

$$F_A = F_{A0}(1 - X_A)$$

Where $X_A$ = Conversion of A. This analysis is referenced to the stoichiometry of equation 3.1. The subscript 0 refers to the feed condition.

Substituting the rate law (equation 3.17) we have already calculated in chapter 3, the balance becomes:

$$\frac{F_{A0}}{A_C}\frac{dX_A}{dZ} = \frac{k_S K_A P_A}{1 + K_A P_A + K_C P_C} \qquad (5.4)$$

Where the notation has been modified such that

$K_A \equiv K_1$ *and* $K_C \equiv K_3$

The molar concentration of gaseous species i is Ci given by:

$$C_i = \frac{F_i}{\upsilon} = \frac{F_{A0}(\theta_i + \nu_i X_A)}{\upsilon_0\left(\frac{P_0}{P}\right)\left(\frac{T}{T_0}\right)(1 + \varepsilon_A X_A)}$$

Where $\upsilon$ = Volumetric flow rate

P = Pressure

T = Temperature

$\nu_i$ = Stoichiometric coefficient

$\theta_i = F_{i0}/F_{A0}$ and

$\varepsilon_A = y_{A0}\,\delta_A$

where $y_{A0}$ = mole fraction of A in the feed

$\delta_A = 1/2 + 1/3 - 1 = -1/6$

Since $y_{A0} <<< 1$ (i.e. HCl very dilute), $\varepsilon_A \approx 0$

Also for assumed constant pressure, the above equation for $C_i$ becomes:

$$C_i \approx C_{A_0}(\theta_i + \nu_i X_A)\left(\frac{T_0}{T}\right)$$

$$P_i = C_i R T = C_{A_0}(\theta_i + \nu_i X_A)\left(\frac{T_0}{T}\right) R T = C_{A_0} R T_0 (\theta_i + \nu_i X_A)$$

Where $P_i$ = Partial pressure of i.

$$P_A = C_{A0} R T_0 (1 - X_A)$$

$$P_C = \frac{1}{3} C_{A0} R T_0 X_A$$

Where R = 82.1 $cm^3$ atm / mol K

The adsorption equilibrium constants are of the form:

$$K_A = \exp\left(\frac{-A'}{R'T}\right)$$

$$K_C = \exp\left(\frac{-C'}{R'T}\right)$$

Where R' = 1.987 cal / mol K .

A', C' are parameters specific to this chemical reaction..

The rate constant for surface reaction can be given by the Arrhenius equation.

$$k_S = A_F \exp\left(\frac{-E_a}{R T}\right)$$

Substituting the values of $P_A$ and $P_C$ equation 5.4 becomes.

$$\frac{F_{A_0}}{A_C}\frac{dX_A}{dZ} = \frac{k_S K_A C_{A_0} R T_0 (1 - X_A)}{1 + K_A C_{A_0} R T_0 (1 - X_A) + \frac{K_C}{3} C_{A_0} R T_0 X_A} \qquad (5.5)$$

Since the adsorption is exothermic, the higher the reaction temperature, the smaller the equilibrium constant. Assuming the temperature is high enough that the concentrations of adsorbed species are relatively low, the denominator simplifies as:

$$1 >>> (P_A K_A + P_C K_C)$$

Hence, the denominator of rate law approaches 1. Equation 5.5 could then be approximated as

$$\frac{F_{A_0}}{A_C}\frac{dX_A}{dZ} \approx k_S K_A C_{A_0} R T_0 (1 - X_A) \qquad (5.6)$$

Substituting $K_A$, $k_S$, equation 5.6 becomes

$$\frac{F_{A_0}}{A_C}\frac{dX_A}{dZ} = A_F \exp\left[\frac{-E_a}{RT}\right].\exp\left[\frac{-A'}{RT}\right] C_{A_0} R T_0 (1 - X_A) \qquad (5.7)$$

This can be integrated after separation of variables:

$$\frac{F_{A_0}}{A_C A_F C_{A_0} R T_0}\int_0^{X_A}\frac{dX_A}{(1 - X_A)} = \int_0^Z \exp\left[\frac{-E_a - A'}{RT}\right] dZ \qquad (5.8)$$

$$-\ln(1 - X_A)\frac{F_{A_0}}{A_C C_{A_0} R T_0} = A_F \int_0^Z \exp\left[\frac{E'}{RT}\right] dZ \qquad (5.9)$$

$$where \qquad E' = -E_a - A'$$

Equation 5.9 is the required mathematical model, which has to be solved in order to get two unknown variables $A_F$ and E'. The other parameters ($F_{A0}$, $A_C$, $C_{A0}$, $T_0$) are known. Temperature T is known a function of Z for the integral. Conversions $X_A$ are determined from the titration data. Unfortunately, the parameters $E_a$ and A' cannot be separated.

# CHAPTER 6

## RESULTS AND CONCLUSIONS

In the previous chapter a mathematical model had been developed to find the kinetic parameters for the reaction between $Sb_2O_3$ and HCl.

$$-\ln(1 - X_A)\frac{F_{A_0}}{A_C C_{A_0} R T_0} = A_F \int_0^Z \exp\left[\frac{E'}{RT}\right] dZ \qquad (5.9)$$

$$let \qquad C \equiv A_F \int_0^Z \exp\left[\frac{E'}{RT}\right] dZ$$

$$where \qquad C = -\ln(1 - X_A)\frac{F_{A0}}{A_C C_{A0} R T_0}$$

The consistency in the values of constant C for the runs performed at same conditions suggests validity of the mathematical model developed and the assumptions made. The fluctuations in the values of C are due to uncertainty in determining conversion as discussed in chapter 2.

Also as

$$C_{A_0} = \frac{F_{A_0}}{\nu_{N_2} + \nu_{HCl}} \approx \frac{F_{A_0}}{\nu_{N_2}}$$

Where $\nu_i$ = volumetric flow rate of species i.

Therefore

$$C = -\ln(1 - X_A)\frac{F_{A_0}}{A_C \frac{F_{A_0}}{\nu_{N_2}} RT_0} = -\ln(1 - X_A)\frac{\nu_{N_2}}{A_C R T_0}$$

So this is clear that molar rate of HCl and the initial concentration ($F_{A0}$ and $C_{A0}$) should have little or no effect on the value of constant C.

The constant C has been calculated for every run and the results are tabulated as below:

**At reactor set point temperature of 300C**

**Table 6.1** $F_{A0}$, $C_{A0}$, $X_A$ and constant C at $N_2$ flow of 0.2 SCFM and dust rate of 0.43 rpm

| RUN # | $N_2$ Flow rate SCFM | $F_{A0}$ | $C_{A0}$ | $T_0$ (C) | $X_A$ | Temperature Profile | C |
|---|---|---|---|---|---|---|---|
| 1 | 0.2 | $1.03 * 10^{-5}$ | $1.8 * 10^{-9}$ | 123 | 0.404 | $T = -0.0309Z^2 + 4.634Z + 398.87$ | 0.2296 |
| 2 | 0.2 | $8.02 * 10^{-6}$ | $1.416 * 10^{-9}$ | 123 | 0.355 | $T = -0.0309Z^2 + 4.634Z + 398.87$ | 0.1925 |
| 3 | 0.2 | $6.02 * 10^{-6}$ | $1.063 * 10^{-9}$ | 123 | 0.37 | $T = -0.0309Z^2 + 4.634Z + 398.87$ | 0.203 |
| 4 | 0.2 | $4.01 * 10^{-6}$ | $7.08 * 10^{-10}$ | 123 | 0.425 | $T = -0.0309Z^2 + 4.634Z + 398.87$ | 0.243 |
| Average | | | | | 0.39 | | 0.217 |

**Table 6.2** $F_{A0}$, $C_{A0}$, $X_A$ and constant C at $N_2$ flow of 0.15 SCFM and dust rate of 0.43rpm

| RUN # | $N_2$ Flow rate SCFM | $F_{A0}$ | $C_{A0}$ | $T_0$ (C) | $X_A$ | Temperature Profile | C |
|---|---|---|---|---|---|---|---|
| 5 | 0.15 | $1.03 * 10^{-5}$ | $2.42 * 10^{-9}$ | 128 | 0.438 | $T = -0.0366Z^2 + 4.973Z + 402.51$ | 0.190 |
| 6 | 0.15 | $8.02 * 10^{-6}$ | $1.888 * 10^{-9}$ | 128 | 0.329 | $T = -0.0366Z^2 + 4.973Z + 402.51$ | 0.132 |
| 7 | 0.15 | $6.02 * 10^{-6}$ | $1.42 * 10^{-9}$ | 128 | 0.36 | $T = -0.0366Z^2 + 4.973Z + 402.51$ | 0.147 |
| 8 | 0.15 | $4.01 * 10^{-6}$ | $9.44 * 10^{-10}$ | 128 | 0.4256 | $T = -0.0366Z^2 + 4.973Z + 402.51$ | 0.183 |
| Average | | | | | 0.39 | | 0.163 |

**Table 6.3** $F_{A0}$, $C_{A0}$, $X_A$ and constant C at $N_2$ flow of 0.15 SCFM and dust rate of 0.55rpm

| RUN # | $N_2$ Flow rate SCFM | $F_{A0}$ | $C_{A0}$ | $T_0$ (C) | $X_A$ | Temperature Profile | C |
|---|---|---|---|---|---|---|---|
| 9 | 0.15 | $1.31 * 10^{-5}$ | $3.08 * 10^{-9}$ | 128 | 0.471 | $T = -0.0366Z^2 + 4.973Z + 402.51$ | 0.210 |
| 10 | 0.15 | $1.03 * 10^{-5}$ | $2.42 * 10^{-9}$ | 128 | 0.47 | $T = -0.0366Z^2 + 4.973Z + 402.51$ | 0.209 |
| 11 | 0.15 | $8.02 * 10^{-6}$ | $1.88 * 10^{-9}$ | 128 | 0.4272 | $T = -0.0366Z^2 + 4.973Z + 402.51$ | 0.184 |
| 12 | 0.15 | $6.02 * 10^{-6}$ | $1.42 * 10^{-9}$ | 128 | 0.3778 | $T = -0.0366Z^2 + 4.973Z + 402.51$ | 0.156 |
| Average | | | | | 0.44 | | 0.189 |

**Table 6.4** $F_{A0}$, $C_{A0}$, $X_A$ and C at $N_2$ flow of 0.15 SCFM and HCl flow of 4.62 ml/min

| RUN # | $N_2$ Flow rate SCFM | $F_{A0}$ | $C_{A0}$ | $T_0$ (C) | $X_A$ | Temperature Profile | Dust rate rpm | C |
|---|---|---|---|---|---|---|---|---|
| 13 | 0.15 | $1.03 * 10^{-5}$ | $2.42 * 10^{-9}$ | 128 | 0.3385 | $T = -0.0366Z^2 + 4.973Z + 402.51$ | 0.20 | 0.136 |
| 14 | 0.15 | $1.03 * 10^{-5}$ | $2.42 * 10^{-9}$ | 128 | 0.4058 | $T = -0.0366Z^2 + 4.973Z + 402.51$ | 0.30 | 0.172 |
| 15 | 0.15 | $1.03 * 10^{-5}$ | $2.42 * 10^{-9}$ | 128 | 0.4179 | $T = -0.0366Z^2 + 4.973Z + 402.51$ | 0.50 | 0.178 |

**Table 6.5** $F_{A0}$, $C_{A0}$, $X_A$ and C at $N_2$ flow of 0.15 SCFM and HCl flow of 2.7 ml/min

| RUN # | $N_2$ Flow rate SCFM | $F_{A0}$ | $C_{A0}$ | $T_0$ (C) | $X_A$ | Temperature Profile | Dust rate rpm | C |
|---|---|---|---|---|---|---|---|---|
| 16 | 0.15 | $6.02 * 10^{-6}$ | $1.42 * 10^{-9}$ | 128 | 0.3086 | $T = -0.0366Z^2 + 4.973Z + 402.51$ | 0.20 | 0.121 |
| 17 | 0.15 | $6.02 * 10^{-6}$ | $1.42* 10^{-9}$ | 128 | 0.377 | $T = -0.0366Z^2 + 4.973Z + 402.51$ | 0.325 | 0.155 |
| 18 | 0.15 | $6.02 * 10^{-6}$ | $1.42 * 10^{-9}$ | 128 | 0.4917 | $T = -0.0366Z^2 + 4.973Z + 402.51$ | 0.450 | 0.222 |
| 19 | 0.15 | $6.02 * 10^{-6}$ | $1.42 * 10^{-9}$ | 128 | 0.5020 | $T = -0.0366Z^2 + 4.973Z + 402.51$ | 0.55 | 0.229 |

**Table 6.6** $F_{A0}$, $C_{A0}$, $X_A$ and C at $N_2$ flow of 0.15 SCFM and HCl flow of 5.87 ml/min

| RUN # | $N_2$ Flow rate SCFM | $F_{A0}$ | $C_{A0}$ | $T_0$ (C) | $X_A$ | Temperature Profile | Dust rate rpm | C |
|---|---|---|---|---|---|---|---|---|
| 20 | 0.15 | $1.31 * 10^{-5}$ | $3.08 * 10^{-9}$ | 128 | 0.3458 | $T = -0.0366Z^2 + 4.973Z + 402.51$ | 0.30 | 0.139 |
| 21 | 0.15 | $1.31 * 10^{-5}$ | $3.08 * 10^{-9}$ | 128 | 0.4276 | $T = -0.0366Z^2 + 4.973Z + 402.51$ | 0.405 | 0.184 |
| 22 | 0.15 | $1.31 * 10^{-5}$ | $3.08 * 10^{-9}$ | 128 | 0.4712 | $T = -0.0366Z^2 + 4.973Z + 402.51$ | 0.55 | 0.210 |

**At reactor set point temperature of 400C**

**Table 6.7** $F_{A0}$, $C_{A0}$, $X_A$ and C at $N_2$ flow of 0.2 SCFM and dust rate of 0.4 rpm

| RUN # | $N_2$ Flow rate SCFM | $F_{A0}$ | $C_{A0}$ | $T_0$ (C) | $X_A$ | Temperature Profile | C |
|---|---|---|---|---|---|---|---|
| 23 | 0.20 | $1.31 * 10^{-5}$ | $2.3 * 10^{-9}$ | 121 | 0.60 | $T= -0.0948Z^2 + 9.699Z + 436.3$ | 0.405 |
| 24 | 0.20 | $1.03 * 10^{-5}$ | $1.80 * 10^{-9}$ | 121 | 0.61 | $T = -0.0366Z^2 + 4.973Z + 402.51$ | 0.417 |
| 25 | 0.20 | $8.05 * 10^{-6}$ | $1.42 * 10^{-9}$ | 121 | 0.58 | $T = -0.0366Z^2 + 4.973Z + 402.51$ | 0.381 |
| Average | | | | | 0.60 | | 0.401 |

Two differential equations have been established for Tables 6.1 and 6.7 using the average values of C for run 1-4 and 23-25 respectively. These values were chosen since the only major difference between the sets of runs is the set point temperature (i.e. actual temperature profiles). These equations are

$$0.2169 = A_F \int_0^{66} \exp\left[\frac{E'}{1.987(-0.0309Z^2 + 4.633Z + 398.87)}\right] dZ \qquad (6.1)$$

$$0.4012 = A_F \int_0^{66} \exp\left[\frac{E'}{1.987(-0.0948Z^2 + 9.699Z + 463.3)}\right] dZ \qquad (6.2)$$

Where $Z = 26$ in $= 66$ cm

$R' = 1.987$ cal. $mol^{-1}$ . $K^{-1}$

After numerical integration, the equations 6.1 and 6.2 were solved simultaneously. The two unknown parameters obtained are:

$A_F = 0.3552$ moles/sec.$cm^2$.atm

$E' = -E_a - A' = -1862$ cal/mole

Or $E_a + A' = 1862$ cal/mole

### 6.1 Observations and Conclusions

In Table 6.1 for runs 1-4, at a dust rate of 0.43 rpm and $N_2$ rate of 0.2 SCFM, the calculated value of average C is 0.217. In Table 6.2 for runs 5-8 at same dust and HCl rates but at reduced $N_2$ rate of 0.15 SCFM, the value of average C has been decreased to 0.163. This is because the drop in $v_{N2}$ gives a corresponding drop in C for same average $X_A$ as predicted by

$$C \approx -\ln(1 - X_A)\frac{v_{N_2}}{A_C R T_0}$$

Also, the slight difference in the temperature profile because of drop in $N_2$ rate is also a reason for the drop in C.

In Table 6.3 for runs 9-12, where the dust rate is raised from 0.43 rpm to 0.55 rpm keeping the $N_2$ rate at 0.15 SCFM, the conversion and average C has been increased from 0.39 to 0.44 and from 0.163 to 0.189 respectively. This clearly indicates that, at higher dust rates the HCl consumption increases.

Table 6.4 for runs 13-15 suggests a monotonic trend that conversion and C increases by increasing the dust rate. Tables 6.5 and 6.6 also confirm this trend.

Comparison of Tables 6.1 and 6.7 shows that by increasing reactor set point temperature from 300C to 400C, a significant increase has been observed in conversion and C.

This is clear from the above observations that, in all of the experimental runs where HCl rate was varied while keeping the dust rate constant, there was no marked effect on conversion and it almost remained constant. But the volumetric rate of $N_2$ will definitely effect conversion and eventually the constant C.

## 6.2 Final Thoughts

The data and the kinetic parameters obtained from this project are important for:

- Facilitating the design of an airborne metals CEM, and
- Enhancing metals detection

The data collected establish whether and under what conditions metal oxides can be converted quantitatively to vapor metal chlorides on a time scale appropriate for real-time continuous analysis. Specific conditions can be established, as HCl concentration, residence time and reaction temperature needed for greater than 99.9% conversion.

Specification will include reactor tube length and diameter, range of HCl concentrations, and available flow rates.

The chemical volatilization step will improve the sensitivity of trace metals analysis in a wide variety of environmental samples by providing an efficient means to separate metals from their matrices and transport them to the actual analyzer. Such enhancement, therefore, goes far beyond just a metals CEM into the analytical laboratory. Current methods of metals analysis, such as flame or plasma systems, have high emission backgrounds, which reduce sensitivity. A chemical volatilization will remove these problems by quantitatively generating volatile metal chlorides, which are easily amenable to low temperature, non-plasma, analysis techniques such as photofragment fluorescence. The volatilization will also enhance transport within the analytical instrument, thus reducing line losses.

# APPENDIX

## SIMULTANEOUS SOLUTION OF EQUATIONS 6.1 AND 6.2 TO FIND UNKNOWN KINETIC PARAMETERS

Equations 6.1 and 6.2 are:

$$0.2169 = A_F \int_0^{66} \exp\left[\frac{E'}{1.987(-0.0309Z^2 + 4.6336Z + 398.87)}\right] dZ \qquad (6.1)$$

$$0.4012 = A_F \int_0^{66} \exp\left[\frac{E'}{1.987(-0.0948Z^2 + 9.699Z + 463.3)}\right] dZ \qquad (6.2)$$

The integral terms in equations 6.1 and 6.2 are solved by the method of Numerical Integration using Trapezoidal rule (two point) which is one of the simplest and most approximate as it uses the integrand evaluated at the limits of integration to evaluate the integral.

$$\int_{X_0}^{X_1} f(X)dX = \frac{h}{2}\left[f(X_0) + f(X_1)\right]$$

Where $h = X_1 - X_0$

Therefor

$$\frac{0.2169}{A_F} = \int_0^{66} \exp\left[\frac{E'}{1.987(-0.0309Z^2 + 4.633Z + 398.87)}\right] dZ$$

$$\frac{0.2169}{A_F} = 33\left[\exp\left(\frac{E'}{1132.74}\right) + \exp\left(\frac{-E'}{792.55}\right)\right]$$

Simplifying and taking log on both sides

$$-5.0248 - \ln A_F = 2.1428 \times 10^{-3} E' \qquad (A)$$

Similarly equation 6.2 will be simplified to:

$$-4.414 - \ln A_F = 1.8148 \times 10^{-3} E' \qquad (B)$$

Solving equations A and B simultaneously:

$$A_F = 0.3552 \ \frac{moles}{sec.cm^2.atm}$$

$$E' = -E_a - A' = E_a + A' = 1862 \ \frac{cal}{mole}$$

# REFERENCES


1. Szekely Julian and Evans W. James, *Gas – Solid Reactions*, Academic Press , New York, 1976.

2. Fogler, Scott, H., *Elements of Chemical Reaction Engineering*, 2nd ed., Prentice-Hall Inc., New Jersey, 1992.

3. Levenspiel Octave, *Chemical Reaction Engineering*, 2nd ed., John Wiley & Sons, Inc., New York, 1989.

4. Smithells J. Colin, *Metals Reference Book*, Vol.1, 4th ed., Plenum Press, New York, 1967.

5. Brodkey S. Robert and Hershey C. Harry, *Transport Phenomena, A Unified Approach*, McGraw-Hill Book Company, New York, 1988.

6. Bird, R. B., *Transport Phenomena*, McGraw-Hill Book Company, New York,

7. Othmer Kirk, *Encyclopedia of Chemical Technology*, Vol.3, 3rd ed., John Wiley and Sons, New York, 1978.

8. Perry, Green, W., *Chemical Engineering Hand Book*, 6th ed., McGraw-Hill Book Company, New York, 1984.

9. R.B.Barat and A.T.Poulos, "Applied Spectroscopy", vol.52, pp 1360+, 1998.

10. R.B.Barat and A.T.Poulos, "Progress Report-R2D2 Project", 1996.

11. WDF-II Operating Instructions, BGI Incorporated, 2nd ed., Waltham, MA, 1989.